1892 *J. Phys. Chem. C* **2010,** *114,* 1892–1900

Computational Study of Carbonyl Sulphide Formation on Model Interstellar Dust Grains

D. A. Adriaens, T. P. M. Goumans,[†] C. R. A. Catlow, and W. A. Brown*

Department of Chemistry, University College London, 20 Gordon Street, London, WC1H 0AJ, U.K.

Received: August 28, 2009; Revised Manuscript Received: November 26, 2009

The formation of carbonyl sulphide, OCS, is investigated computationally on a model carbonaceous grain surface (coronene) using density functional theory. Four reaction pathways for the formation of OCS are investigated: formation from CO + S (on both the singlet and the triplet surfaces) and CO + HS, and formation from CS + O (again on both the singlet and the triplet surfaces) and CS + OH. The Langmuir−Hinshelwood, Eley−Rideal, and hot-atom mechanisms are investigated. Calculations show that all species in the ground state are physisorbed on the surface. However, both sulfur and oxygen in their first excited states chemisorb on coronene. The first reaction pathway, ^{3}OCS formation from CO + ^{3}S, is activated by 18.7 kJ mol^{-1} in the gas phase. This barrier is much too high for the reaction to occur at a significant rate at the low temperatures (10−20 K) found in dark interstellar clouds. However, calculations show that coronene catalyzes this reaction, lowering the barrier to 15.6 kJ mol^{-1} for the Langmuir−Hinshelwood reaction and to 7.1 kJ mol^{-1} for the Eley−Rideal reaction compared with the same reaction in the gas phase. For the similar reaction CS + ^{3}O → ^{3}OCS, the gas-phase activation barrier is negative, and it remains so on a coronene surface. The formation of OCS from CO + HS does not take place in a one-step mechanism. Instead, a stable intermediate (HSCO) is formed on the surface, which can subsequently react with a hydrogen atom to form OCS and H_2. Finally, CS + OH can react to form a hot HOCS intermediate, which can either react exothermically to yield H + OCS or be stablised on the surface. In the latter case, reaction with another H atom can yield H_2 + OCS.

1. Introduction

Grain particles play an essential role in interstellar chemistry.[1−3] The exact composition of the dust grains remains unknown, although there is strong evidence that they are composed of carbonaceous or siliceous material.[1−5] Depending on the region, the grains may also be covered in ices. Polycyclic aromatic hydrocarbons (PAHs), or agglomerations thereof, are thought to be a good candidate for the main component of carbonaceous dust grains.[1,4] The importance of surface chemistry has already been shown for H_2-formation (for example, refs 6 and 7 and references therein), where dust grains have been found to catalyze the process. Other molecules[8,9] are also thought to be formed on the grain surface, and experiments on models of these grains and investigations of their impacts on chemistry under conditions relevant to the interstellar medium (ISM) have been performed (for example, refs 9−12).

Atoms and molecules can agglomerate on a dust particle, and hence, some reactions are more likely to take place on dust compared to in the gas phase. In this paper, we present the results of an investigation of carbonyl sulphide (OCS) formation on coronene using density functional theory (DFT). Coronene, $C_{24}H_{12}$, is considered to be a good model for PAHs, and it has been used previously as the minimal model to model graphite, graphene, or PAHs.[13−18] Coronene is large enough that it does not have hydrogen interactions or other side-effects (e.g., for the smaller benzene molecule, the hydrogen atoms have a strong influence on the surface−adsorbate interaction) but not so big that it cannot be treated quantum chemically. In the calculations performed here, it was always ensured that reactants and products were bound to the central six carbon atoms of the coronene so that any possible edge effects were eliminated.

Sulfur-bearing species have been proposed as good evolutionary chemical tracers of star-forming regions.[19] Their abundances vary by substantial amounts during the evolution of a protostar; therefore, astronomical models are very sensitive to the amount of sulfur present and to its chemical composition.[19] However, uncertainties regarding the form that sulfur takes once it depletes from the grains, as well as its highly reactive nature,[20] mean that particular attention must be paid to surface reactions involving sulfur.

The most abundant species found in the ISM are hydrogen atoms, and hence, it is often assumed that hydrogenation is the most likely surface reaction occurring during the formation of a star. However, the situation seems to be more complex for sulfur reactions on grains, because there has been no detection of H_2S ices.[21,22] The failure to detect these ices and the detection of solid OCS[23] have raised the possibility that OCS may be one of the main reservoirs of sulfur on the grains.[24] However, the exact formation pathways leading to OCS, and their relative contribution to OCS formation, are still unknown. Many other sulfur-bearing species have also been detected in the ISM, including CS, NS, SO, SO_2, C_2S, H_2CS, and C_3S.

Previous studies of OCS formation and reaction, both experimental and theoretical, have been mostly limited to the gas phase.[25−31] Rice et al.[26−28] and Häusler et al.[31] studied the reaction of OCS with a hydrogen or deuterium atom. In contrast, Sayós et al.[29] investigated the reaction of CS + ^{3}O → ^{3}OCS → CO + ^{3}S. There has been one previous experimental study of OCS formation under interstellar conditions. Ferrante and coworkers[32] showed that OCS can be readily formed in the solid state from the proton irradiation of ices containing various mixtures of CO, CO_2, H_2S, and SO_2. Although this study did not investigate the energetics of OCS formation, they concluded

---

* Corresponding author. E-mail: w.a.brown@ucl.ac.uk.

[†] Present address: Gorlaeus Laboratories, Leiden Institute of Chemistry, Leiden University, P.O. Box 9502, 2300 RA Leiden, The Netherlands.

10.1021/jp9083212

that OCS was formed by the reaction of CO with free S, generated from the proton-induced fragmentation of the parent S-containing species. The formation of *trans*-HSCO, a possible intermediate in OCS formation, has also been observed in studies of the ultraviolet irradiation of H_2S and CO in an Ar matrix.[33]

In this study, we have investigated OCS formation via four reaction pathways which have been grouped according to the source of the reactants (H_2S or H_2O):

$$CO + S \rightarrow OCS \tag{1}$$

$$CO + HS \rightarrow OCS + ... \tag{2}$$

$$CS + O \rightarrow OCS \tag{3}$$

$$CS + OH \rightarrow OCS + ... \tag{4}$$

All reaction pathways for OCS formation have been investigated computationally in the gas phase and on coronene. To benchmark the DFT calculations, we compare our gas-phase calculations with previous results and with high-level ab initio calculations also performed in this study. For the first and third reactions, it is important to look at both singlet and triplet states because the ground states of reactants and products differ in spin state. Hence, reactions on both the singlet and the triplet surface were examined for these reactions. The second and fourth reactions are in fact multistep reactions. The complete reaction pathways studied are therefore as follows:

$$CO + {}^1S \rightarrow {}^1OCS \tag{1a}$$

$$CO + {}^3S \rightarrow {}^3OCS \tag{1b}$$

$$CO + HS \rightarrow cis\text{-}HSCO \rightarrow OCS + H \tag{2a}$$

$$CO + HS \rightarrow trans\text{-}HSCO \rightarrow OCS + H \tag{2b}$$

$$CO + HS \rightarrow cis\text{-}HSCO(+H)\ \text{addition} \rightarrow OCS + H_2 \tag{2c}$$

$$CO + HS \rightarrow trans\text{-}HSCO(+H)\ \text{addition} \rightarrow OCS + H_2 \tag{2d}$$

$$CS + {}^1O \rightarrow {}^1OCS \tag{3a}$$

$$CS + {}^3O \rightarrow {}^3OCS \tag{3b}$$

$$CS + OH \rightarrow \text{cis-HOCS} \rightarrow OCS + H \tag{4a}$$

$$CS + OH \rightarrow trans\text{-}HOCS \rightarrow OCS + H \tag{4b}$$

$$CS + OH \rightarrow cis\text{-}HOCS(+H) \rightarrow OCS + H_2 \tag{4c}$$

$$CS + OH \rightarrow trans\text{-}HOCS(+H) \rightarrow OCS + H_2 \tag{4d}$$

O and OH are essential reactants in reactions 3 and 4 and, on the dust grain, can be formed in situ via photodissociation of H_2O by either ultraviolet or cosmic-ray irradiation. Reaction of a hydrogen-bearing radical with an oxygen-bearing species (e.g., CH + O_2, CH_2 + O, CH_2 + O_2, O + HCO)[34] is also another possibility to yield OH. Similarly, S and HS, required for reactions 1 and 2, find their origin in photodissociated H_2S or reaction of a hydrogen-bearing radical with a sulfur-bearing molecule.

TABLE 1: Comparison of DFT and Ab Initio Gas-Phase Reaction Energies for a Selection of the Reactions Considered for OCS Formation in this Study

	reaction energy/ kJ mol^{-1}	
reaction	MPWB1K 6-311G**	CCSD(T)/CBS
CO + ^{3}S → ^{3}OCS	6.9	9.8
CS + ^{3}O → ^{3}OCS	–359.3	–361.7
CO + HS → *trans*-HSCO	–13.7	–19.0
CO + HS → *cis*-HSCO	–4.9	–9.3
trans-HSCO → *cis*-HSCO	8.8	9.8
CS + OH → *trans*-HOCS	–260.2	–254.1

2. Computational Details

All of the DFT calculations have been performed using the Gaussian03 package,[35] with those for all gas-phase species having been benchmarked against high-level ab initio calculations also performed in this study, to ensure the accuracy of the results. The ab initio values were calculated with Molpro[36] with CCSD(T) energies extrapolated to the complete basis set (CBS) limit with aug-cc-pVTZ and aug-cc-pVQZ bases on CCSD(T)/aug-cc-pVTZ optimized geometries. DFT has been used to optimize the geometry of all of the reactants, products, and intermediates: H, ^{3}S, ^{1}S, ^{3}O, ^{1}O, H_2, CO, CS, HS, OH, H_2S, H_2O, *cis*-HSCO, *trans*-HSCO, iso-HSCO, *cis*-HOCS, *trans*-HOCS, and OCS in both the singlet and the triplet state, denoted ^{1}OCS and ^{3}OCS. All of the species were optimized both in the gas phase and adsorbed on coronene. Within the DFT scheme, the MPWB1K functional was chosen, because it has been optimized for the computation of barrier heights and weak interactions[37] such as van der Waals interactions. Saddle-point geometries were optimized from initial structures obtained by constrained potential-energy surface scans along the reaction coordinate or via quadratic synchronous transit. The nature of all reactants, products, and transition states was assured by checking the number of imaginary frequencies. All reaction energies and activation barriers are given in kJ mol^{-1}, and zero-point energy corrections have been applied to all DFT results.

In previous work,[38] it was found that, depending on the basis set and Hamiltonian used, coronene can have an imaginary vibrational frequency. This problem has also been observed for other small aromatic molecules,[39,40] but given that these molecules are stable, it is likely that this is an artifact arising from diffuse Gaussian functions in the basis set and that these functions in a Pople basis set should be avoided. Hence, a basis set without diffuse functions (the 6-311G(d,p) Pople basis set) was used for the calculations described here. This was found to eliminate the problem.

Table 1 shows a comparison between gas-phase reaction energies calculated with the MPWB1K functional and high-level ab initio calculations at the CCSD(T)/CBS level for a selection of the most important reactions investigated in this study. It is clear that there is good agreement between the DFT and ab initio values, showing that the MPWB1K functional with a 6-311G** basis set is suitable for the calculations presented here. We have previously used the same methods and functionals

TABLE 2: Calculated and Experimental Reaction Energies and Activation Barriers for Gas-Phase and Coronene-Catalysed OCS Formation from CO + S and CS + O via the LH and ER Mechanisms[a]

	energy/ kJ mol^{-1}						
	gas-phase reactions					reactions on coronene	
molecule/reaction	this study	Hijazo[25]	Sayós et al.[29]	Gonzales et al.[30]	experimental value	LH this study	ER this study
$CO + {}^1S \rightarrow {}^1OCS$	–470.0				–413.5	–301.0	–472.3
activation barrier	no					50.6	No
$CO + {}^3S \rightarrow {}^3OCS$	6.9	40.2	–144.3			0.8	–7.7
activation barrier	18.7	43.4	6.7			15.6	7.1
$CO + {}^3S \rightarrow {}^1OCS$	–301.3				–303.0	–297.7	–303.5
$CS + {}^1O \rightarrow {}^1OCS$	–946.5				–851.7	–558.7	–947.9
activation barrier	no						no
$CS + {}^3O \rightarrow {}^3OCS$	–359.3	–364.34	–577.4	–379.1		–364.2	–370.0
complex (see text)	–3.7						
activation barrier	–2.7	26.28	50.6	9.5	6.3[42]		
$CS + {}^3O \rightarrow {}^1OCS$	–667.5				–661.8	–662.7	–666.0

[a] The table also shows a comparison with the results of previous calculations[25,29,30] and experimentally determined values (CCCBDB, Gurvich 1989, Cox 1989, and Lilenfeld and Richardson).[42]

to study CO_2 formation on coronene,[38] again showing the suitability of the methods used in the present study.

3. Results and Discussion

As noted, both gas-phase and coronene-catalyzed reactions were investigated. The importance of gas-phase reactions is three-fold: the functionals used can be benchmarked against our own ab initio results, they can be validated with previously published experimental and theoretical results, and finally, coronene-catalyzed values can be compared with the gas-phase values to show how large the catalytic influence of the model coronene surface is.

Three types of surface reactions were studied: the Langmuir–Hinshelwood mechanism (LH), the Eley–Rideal mechanism (ER), and the hot-atom mechanism (HA).[41] When both reacting species are on and in thermal equilibrium with the surface, this is the LH reaction. If one of the reactants comes from the gas phase, adsorbs on the surface, and then reacts with the second reactant before it equilibrates with the surface, the HA mechanism is operative. Finally, in the ER mechanism, only one of the reactants is on the surface, and the second one reacts with it directly from the gas phase.

3.1. Gas-Phase Reactions.

Gas-phase calculations were performed and compared with high-level calculations from this study (see Table 1) and with previous results by the Sayós group at different levels of theory.[25,29,30] The calculations by Hijazo et al.[25] were performed at the MP2/6-311(2d) level, and those by Sayós et al.[29] and Gonzales et al.[30] were performed using semiempirical methods at the MNDO/CI level[29] and at the MP4 level.[30] Comparison of our results for OCS formation from CO + S and CS + O with previous results is presented in Table 2. Good agreement was found with experimental values from the online CCCBDB resource (Data from CCCBDB: The Computational Chemistry Comparison and Benchmark Database, http://cccbdb.nist.gov/)[43−46] and from Lilenfeld and Richardson[42] for those reactions where experimental values are available. Again, these results show that the functional and methods used here are suitable for such calculations, as noted by previous work.[37,38]

There is, however, some disagreement between the calculations performed here and previous calculations. In previous investigations of gas-phase OCS formation and reaction, Hijazo et al.[25] studied theoretically the potential energy surface of $CS + O \rightarrow OCS \rightarrow CO + S$. They found that ${}^1OCS$ is more stable than either $CS + {}^1O$ or $CO + {}^1S$. They also reported that the reaction of $CO + {}^3S$ goes via the formation of ${}^3OCS$, which is more stable than $CS + {}^3O$ but less stable than $CO + {}^3S$ or ${}^1OCS$. They found the transition state for ${}^3OCS$ formation from reaction 1b to be very close to ${}^3OCS$, leaving a very small or zero activation barrier for dissociation of ${}^3OCS$ to give $CO + {}^3S$. Similarly, the transition state of reaction 3b is reported to be close to $CS + {}^3O$, making the activation barrier very small. Although these results agree with those in the present study, there are some differences in the exact values of reaction and activation energies, which are probably due to the different methods used. However, because our value of ${}^1OCS$ formation from ${}^3S + CO$ is much closer to the experimental value, we consider our method to be more accurate. The results reported here are in disagreement with two other theoretical studies,[29,47] but the reaction energy is in good agreement with Gonzales et al.[30] However, Sayós et al.,[29] who reported an activation energy for the reaction $CO + {}^3S \rightarrow {}^3OCS$ of only 6.7 kJ mol^{-1} and an activation energy for the reaction $CS + {}^3O \rightarrow {}^3OCS$ of 50.6 kJ mol^{-1}, used semiempirical methods which are generally less accurate than DFT calculations used here. DFT calculations are also expected to be much more accurate than the early calculations of Shapiro et al.[47] performed using the half-collision model. Both groups found that ${}^3OCS$ was much more stable than either $CS + {}^3O$ or $CO + {}^3S$, the latter being in contradiction with our findings.

The formation of OCS starting from CO and HS was also calculated in the gas phase and was compared with previous results, shown in Table 3. The gas-phase calculations show that the overall reaction of $CO + HS \rightarrow OCS + H$ is endothermic by 42.1 kJ mol^{-1} and will thus not occur at 10−20 K. The reaction, however, yields two isomeric HSCO intermediates, which are shown in Figure 1: *cis*-HSCO (where H and O are on the same side of the S—C bond) and *trans*-HSCO (where H and O are on opposite sides of the S—C bond). There is no reaction pathway toward *iso*-HSCO (where H, S, and O are bound to carbon), because there is a large activation energy (>100 kJ mol^{-1}) to the formation of this isomer. This third

TABLE 3: Relative Energies and Activation Energies for Gas-Phase, LH Coronene-Catalysed, and ER Coronene-Catalysed Reactions for OCS Formation from CO + HS and CS + OH[a]

	reaction energy/kJ mol^{-1}				
	gas-phase reactions		reactions on coronene		
molecule/reaction	this study	Rice et al.[28]	LH	ER	HA
$CO + HS \rightarrow OCS + H$	42.1	37.7			
$CO + HS \rightarrow$ *trans*-HSCO	–13.7	–21.8	–19.3	–26.2	–26.2
Activation barrier	6.7	1.7	3.3	via *trans*	–3.6
trans-HSCO $\rightarrow H + OCS$	55.7	59.4			
trans-HSCO $+ H \rightarrow H_2 + OCS$	–477.2				
$CO + HS \rightarrow$ *cis*-HSCO	–4.9	–13.0	–2.8	–9.7	–9.7
Activation barrier	15.4	7.1	16.2	13.3	9.3
cis-HSCO $\rightarrow H + OCS$	47.0	50.6			
cis-HSCO $+ H \rightarrow H_2 + OCS$	–468.5				
trans-HSCO $\rightarrow$ *cis*-HSCO	8.7	8.8			
	32.0	30.5			
$CS + OH \rightarrow OCS + H$	–266.3	–252.7			
$CS + OH \rightarrow$ *trans*-HOCS	–260.2	–248.7	–267.6	–267.1	–267.1
Complex	–10.8	–12.6			
Activation barrier	–7.2	–9.6	submerged	submerged	submerged
trans-HOCS $\rightarrow H + OCS$	via *cis* (–6.2)	–3.8			
trans-HOCS $+ H \rightarrow H_2 + OCS$	–427.6				
$CS + OH \rightarrow$ *cis*-HOCS	–259.7	–246.9			
Activation barrier	via *trans*	no			
cis-HOCS $\rightarrow H + OCS$	–6.7	–5.9	6.1	5.5	
Activation barrier	86.8	63.2	94.7		
cis-HOCS $+ H \rightarrow H_2 + OCS$	–428.1		–415.4	–416.0	
trans-HOCS $\rightarrow$ *cis*-HOCS	0.5	2.1	5.6		
	39.2	38.1	39.6		

[a] Via *cis* and via *trans* reactions have an activation barrier which is much higher than that of their respective variants; therefore, the reaction is more likely to happen when using the other pathway. This also applies to the formation of *trans*-HSCO which will be formed via the LH mechanism. ZPE B3LYP/6-311+G(2df,2p) values of Rice et al.[28] are included for comparison.

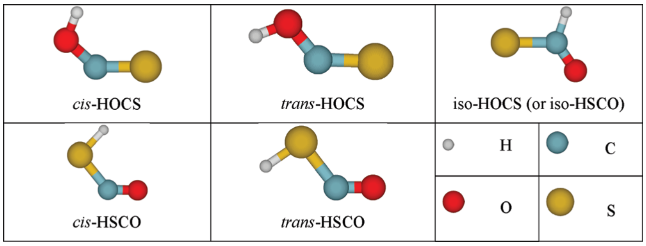

Figure 1. The different isomers of the HSCO and HOCS intermediates as observed in this study. All molecules are planar.

isomeric form of HSCO was, however, reported in the studies of Rice et al.[26−28] Similar isomers are found for the reaction of CS + OH, also shown in Figure 1.

As shown in Table 3, Rice et al.[26−28] performed extensive investigations of the formation and destruction of OCS. Their studies showed that the reaction of $CO + HS \rightarrow H + OCS$ is endothermic. In their work,[26−28] they used several methods (both ab initio and DFT) and basis sets, and hence, they reported a wide range of energies. Their overall reaction energies for the reactions 2a and 2b ranged from 1.3 to 66.5 kJ mol^{-1}. However, their reported B3LYP value[28] (shown in Table 3) of 37.7 kJ mol^{-1} is in good agreement with the results of the present study. Their overall reaction barriers for the reaction of CO + HS were of the order of 43.9−61.5 kJ mol^{-1}, and their reported B3LYP value[28] (again shown in Table 3) was 59.4 kJ mol^{-1}, also very close to the value calculated here. As shown in Table 3, there is very good agreement between our calculated values and the DFT (B3LYP) values reported by Rice.[28] Experimental studies of the same reaction,[31,48,49] performed using hydrogen or deuterium, obtained reaction barriers in the range from 41 to 43 kJ mol^{-1}.

Figures 2 and 3 show the energies for OCS formation for reactions 2 and 4, respectively, including the different isomeric forms of both HSCO and HOCS, and the activation energy needed for one isomer to convert into the other; the calculated values are reported in Table 3. Because the activation barriers to form *iso*-HSCO or *iso*-HOCS are very large, no further reactions involving *iso*-HSCO or *iso*-HOCS were calculated.

There are generally three possibilities when HSCO or HOCS are formed in the gas phase: spontaneous dissociation into OCS and a hydrogen atom (reactions 2a, 2b, 4a, and 4b); further reaction of the intermediate with another hydrogen atom (forming OCS and H_2, reactions 2c, 2d, 4c, and 4d); or dissociation to reform the initial reactants. It is clear from the energies in Table 3 that HSCO, formed from CO + HS, will not spontaneously dissociate into OCS and a hydrogen atom. It is relatively stable and will only react when another species hits it, such as another hydrogen atom. The reaction of HSCO with another hydrogen atom is barrierless and very favorable and strongly drives the reaction (see Table 3), because the formation enthalpy of H_2 as calculated here is -421.5 kJ mol^{-1}. Reaction of HSCO with a hydrogen atom can also lead to the formation of H_2S and CO rather than OCS and H_2. However, although reaction of the HSCO intermediate with an incoming H atom is possible on a surface (see later), it is highly unlikely in the gas phase in the ISM, because it requires a three-body collision. It is therefore much more likely that HSCO, formed in the gas phase, will dissociate to reform the reactants.

The HOCS intermediate can, however, spontaneously dissociate into OCS and a hydrogen atom. This dissociation has an activation barrier of 86.8 kJ mol^{-1}, but the formation energy of *cis*-HOCS is -259.7 kJ mol^{-1}. The OH + CS reaction could therefore proceed immediately to form H and OCS, from the intermediate HOCS.

3.2. Grain-Catalyzed Reactions. ***3.2.1. Adsorption Energies.*** Dust grains can have many effects on the molecules and atoms that adsorb on their surface. In particular, grain surfaces can catalyze reactions and act as heat sinks for excess energy generated during bond-formation reactions. As important as both of these effects, especially under the extreme ISM conditions, is the ability of the surface to adsorb the atoms and molecules,

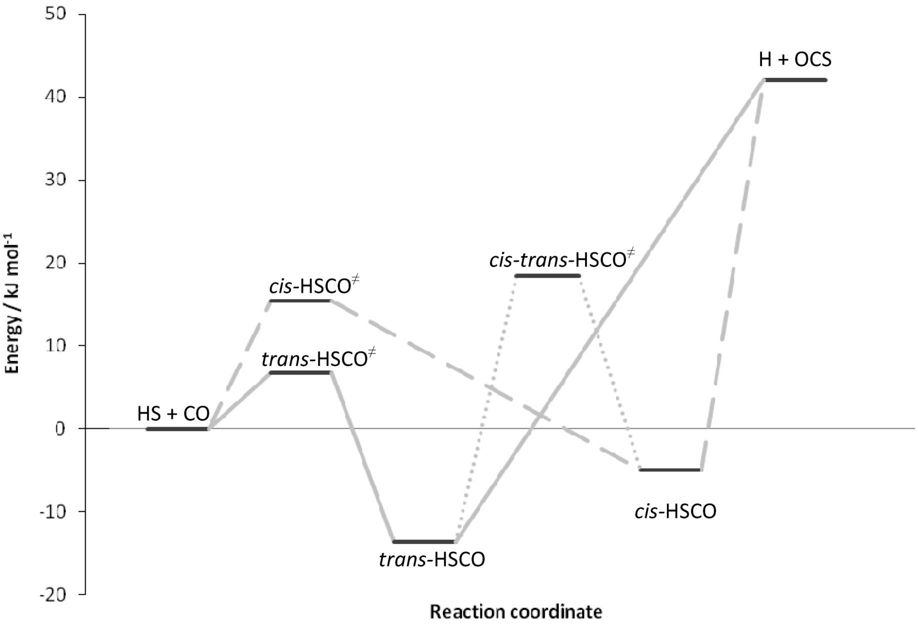

Figure 2. Reaction energy path for OCS formation from HS and CO. The energies shown on the graph are valid for the gas-phase, ER, and LH reactions. The effective values for the gas-phase, LH, and ER reactions are reported in Table 3.

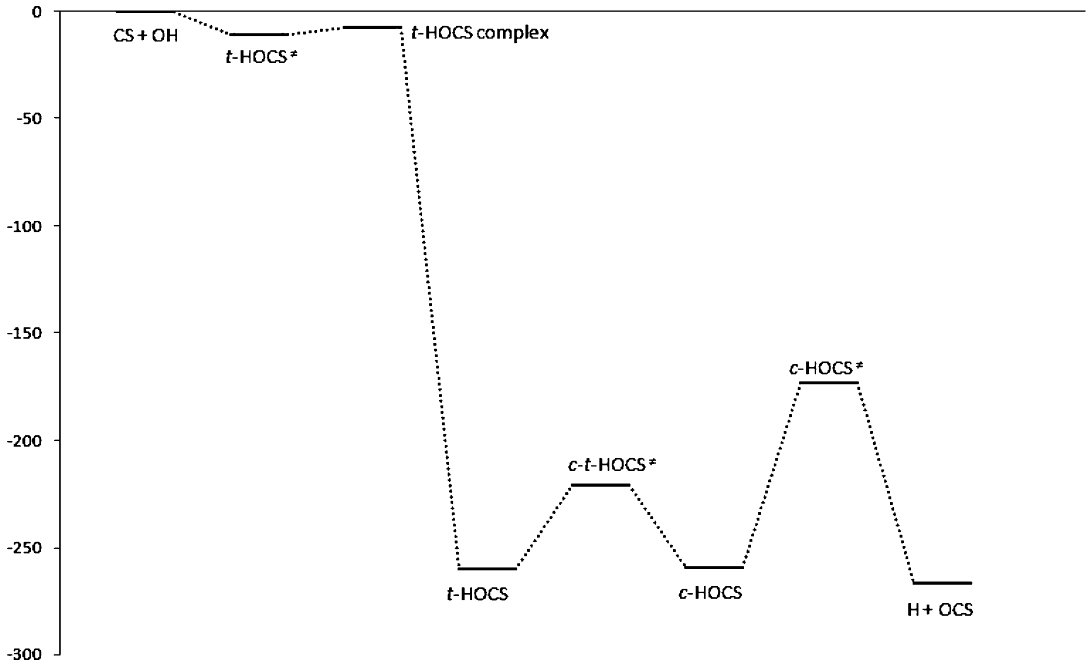

Figure 3. Gas-phase reaction energy path for OCS formation from CS and OH. The energies shown on the graph are valid for the gas-phase, ER, and LH reactions. The effective values for the gas-phase, LH, and ER reactions are reported in Table 3.

TABLE 4: Calculated Adsorption Energies for Atoms and Molecules Important in OCS Formation, Adsorbed on Coronene

	adsorption energy/kJ mol^{-1}
^{1}S	–173.6
^{3}S	–8.6
^{1}O	–388.9
^{3}O	–5.9
CS	–6.3
CO	–2.6
HS	–6.9
OH	–8.5
H_2	+2.6
H_2S	–6.2
H_2O	–9.4
^{1}OCS	–7.5
^{3}OCS	–17.2
cis-HSCO	–7.4
trans-HSCO	–15.1
cis-HOCS	–17.1
trans-HOCS	–22.2

thereby increasing the concentration of the reactants compared to the case in the gas phase. Table 4 shows the adsorption energies for all atoms, molecules, and intermediates on coronene. The results suggest that both molecules and radicals accumulate on the coronene model surface at the temperatures in the ISM, to react eventually to form other products.

The calculated adsorption energies are significantly smaller than experimentally determined values.[50−53] For example, the adsorption energy of CO on graphite is experimentally determined to be between 11 and 13 kJ mol^{-1},[50] whereas our calculations show an adsorption energy of only 2.6 kJ mol^{-1}. A similar difference is found for the H_2 adsorption energy: the experimental value is 5 kJ mol^{-1},[52,53] whereas the present calculations show a repulsion of 2.6 kJ mol^{-1}. This discrepancy is due to the fact that the measured values also include interadsorbate interactions on the surface, as well as an underestimation of weak physisorption interactions by the MPWB1K functional. The nature of the surface also plays an important role. This study investigates adsorption on perfect coronene, whereas the experimental work used graphite, which will contain defects which are expected to have a large effect on adsorption energies.[54,55] We note that, because our computational model underestimates physisorption energies, any effect we do find on catalysis may be greater if the true, stronger interaction is considered. Where our model predicts a positive catalytic effect, we expect that the actual barrier may be reduced because of a stronger interaction with the surface and could be enhanced for certain reactions. Thus, every reaction activation barrier given here can be seen as an upper boundary of the effective barrier.

3.2.2. *Grain-Catalyzed OCS Formation from CO + S.* The coronene-catalyzed reaction energies of CX + Z → OCS (X and Z are either O or S) are shown in Table 1. For the ground-state coronene-catalyzed LH reaction of CO + ^{3}S, there is a reduction of the activation energy for ^{3}OCS formation when compared to that found in the gas phase. The barrier for the reaction on coronene is 15.6 kJ mol^{-1} compared to 18.7 kJ mol^{-1} for the gas-phase reaction. This barrier is reduced even further, down to 7.1 kJ mol^{-1}, for an ER reaction. The reaction also becomes exothermic for the ER reaction, making it feasible in the ISM. The HA mechanism, where one adsorbate is assumed to have its adsorption energy available for reaction, also has an activation barrier of 7.1 kJ mol^{-1}. The LH barrier is still too high for the reaction to occur efficiently in the ISM; but both the ER and the HA activation barriers are sufficiently low for the reaction to happen. In addition, because all mechanisms including the LH mechanism show a reduction of the barrier, resulting from the physisorption of species on coronene, it is clear that our model grain surface does have a catalytic effect on OCS formation.

As already discussed, in the studies reported here, the calculated adsorption energies are lower than the experimental ones. A better description of the van der Waals interactions would give rise to stronger physisorption, and this may lead to an enhanced catalytic effect for the CO + ^{3}S reaction. This is particularly likely because the catalytic effect of coronene on this reaction is most likely due to polarization and weakening of the CO bond by induced-dipole−induced-dipole interactions which would be enhanced by stronger binding of the CO to the surface. Moreover, because some researchers have proposed that dust grains are negatively charged,[55,56] it is plausible to assume that coronene may also be negatively charged. Preliminary results investigating this effect suggest that molecules physisorb more strongly on negatively charged coronene than on neutral coronene and are therefore likely to reduce the activation barrier for OCS formation even further.

Coronene also has another important effect on the reaction between CO and ^{3}S. Coronene, and indeed any other dust grain, can act as a heat sink for excess energy generated during OCS formation. CO reacting with ground state sulfur (^{3}S) will initially form OCS in an excited triplet state ($^3\Sigma$). OCS in such an excited state easily reacts back to give CO and S. On the coronene surface, however, ^{3}OCS is stabilized by physisorption (17.2 kJ mol^{-1} adsorption energy, compared to 11.1 kJ mol^{-1} for CO and ^{3}S combined) and can therefore relax to its ground state ($^1\Sigma$) by intramolecular energy transfer, allowing OCS formation.

Coronene also acts as a heat sink for the reaction of ^{1}S with CO to form OCS. Starting from the singlet state (^{1}S), sulfur is chemisorbed on the coronene surface (adsorption energy 173.6 kJ mol^{-1}). The LH reaction of CO + ^{1}S to form ^{1}OCS is therefore strongly activated and hence will have a low probability of occurring. However, reaction of CO_{ads} + $^1S_{gas}$ following either the ER or the HA mechanism is barrierless and has a high probability. Here again, the heat-sink effect of coronene is very important, because the reaction releases −270.0 kJ mol^{-1} of excess energy. The efficiency of the heat-sink effect depends on the exact dynamics of the system.

3.2.3. *Grain-Catalyzed OCS Formation from CS + O.* In addition to the CO + S energies, Table 2 shows the energies for OCS formation starting from CS and atomic oxygen. We note first of all that, even though this reaction looks similar to the previous reaction (CO + S), the reactions are in fact quite different. Atomic oxygen forms a van der Waals complex with CS, which will lead to activation barriers which have a lower energy than those of the reagents. In both Tables 2 and 3, these are referred to as negative barriers (e.g., refs 57 and 58). It is noted that these types of reactions can be fast at very low temperatures and could display complex kinetic behavior such as both negative and positive Arrhenius activation energies at low and high temperatures, respectively.[59−61] Hence, the barriers are easily overcome, even in the ISM. This effectively means that, in the case of CS + ^{3}O, an intermediate complex is formed (yielding 3.7 kJ mol^{-1} of energy), which will immediately react to ^{3}OCS, thereby passing through the transition state which is 1.0 kJ mol^{-1} higher in energy than this complex. Thus, with respect to the original reactants, the transition state is 2.7 kJ mol^{-1} lower in energy. Obviously, even though the influence of a surface can still further reduce this barrier, the adsorption

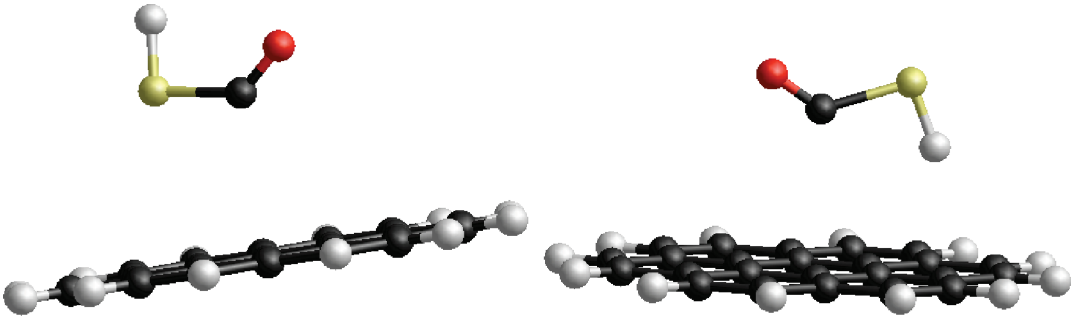

Figure 4. Most-stable orientations of *cis*-HSCO (left) and *trans*-HSCO (right) adsorbed on coronene.

of CS and O onto this surface is of much greater importance because this reaction would occur even in the gas phase. The adsorption energy of CS is more than twice as large as that of CO; thus, desorption will be less effective, leading to a higher reaction rate, as explained below. The heat-sink effect of the surface is also important because the reaction yields more than twice as much energy compared with the CO + S reaction.

3.2.4. Grain-Catalyzed OCS Formation from CO + HS.

Trans-HSCO has been detected previously,[33] upon bombardment of a mixture of H_2S and CO in an argon matrix. This evidence supports the theoretical calculations which show that *trans*-HSCO is relatively stable on a surface.

The LH formation of *cis*-HSCO from CO + HS on coronene is activated by 16.2 kJ mol^{-1}, as shown in Table 3. Conversely, a similar formation mechanism for *trans*-HSCO only requires an activation barrier of 3.3 kJ mol^{-1}. It is therefore very likely that *trans*-HSCO formation will dominate in the ISM. The activation barrier for the formation of *trans*-HSCO is much lower in the LH mechanism. HS will therefore most likely physisorb before reaction (following the LH mechanism), rather than reacting immediately (following the ER mechanism). The HA mechanism predicts a negative activation barrier, signifying that more energy is available from adsorbing the HS molecule than is required to overcome the activation barrier.

Figure 4 shows the orientation of *cis*- and *trans*-HSCO on coronene. Although both isomers of HSCO are relatively stable on the coronene surface, they can dissociate to give H + OCS or react with a hydrogen atom to yield either OCS or H_2S. The reaction energies in Table 3 show that spontaneous dissociation into OCS and a hydrogen atom is always unfavorable for both *cis*- and *trans*-HSCO, both in the gas phase and on a surface, with a minimum reaction energy of 47.0 kJ mol^{-1}. Therefore, although the HSCO intermediate from the HS + CO reaction is likely to redissociate to the reactants in the gas phase, this complex may be stabilized on the surface of a dust grain. As mentioned above, HSCO can react further with another hydrogen atom, forming either H_2 + OCS or H_2S + CO. The H—S bond energy in H_2S is around 350 kJ mol^{-1}, and the H_2 bond energy is over 400 kJ mol^{-1}; therefore, reaction of HSCO with a hydrogen atom will be very exothermic. Following the formation of H_2 and OCS from H and HSCO, it is very likely that much of the formation energy will go into rovibrationally excited H_2, which means that, even though ^{3}OCS will be formed in an excited state, it will probably not dissociate back into CO and S. The reaction of HSCO with a hydrogen atom to yield either H_2S and CO or OCS and H_2 is barrierless in both cases. Hence, only the formation of an HSCO intermediate is important in determining whether OCS will be formed on coronene via the CO + HS reaction. The branching ratio will be determined by the detailed dynamics of the H + HSCO reaction, which will depend strongly on the angle of approach of the incoming hydrogen atom.

3.2.5. Grain-Catalyzed OCS Formation from CS + OH.

Contrary to the formation of HSCO, the HOCS intermediate can immediately dissociate to give OCS and a hydrogen atom without the need for a second hydrogen atom to abstract the first one. Like with the reaction of CS + ^{3}O, an intermediate complex is formed, which then leads to *trans*-HOCS. The gas-phase activation barrier toward *trans*-HOCS is only 3.6 kJ mol^{-1}, which can easily be overcome by the 10.8 kJ mol^{-1} of energy released upon formation of the complex. *Trans*-HOCS will subsequently isomerize to *cis*-HOCS; this isomerization has an activation barrier of 39.2 kJ mol^{-1} in the gas phase. *Cis*-HOCS can consequently dissociate into OCS and H. For gas-phase *cis*-HOCS, the activation energy to form OCS spontaneously is 86.8 kJ mol^{-1}, which is still much less than the residual energy of 260.2 kJ mol^{-1}, released upon formation of *trans*-HOCS. It is likely that the energy transfer to the surface phonon modes is slower than the transfer to internal molecular rotations and vibrations. If less than the excess formation energy (approximately 175 kJ mol^{-1}) is transferred to the surface, it is possible for spontaneous dissociation to take place.

The catalytic influence of coronene on the CS + OH reaction is, hence, similar to that in the CS + O reaction: the activation barrier is negative, and thus, the adsorption of the species and the third-body effect are more important than any lowering of the activation barrier. However, we also note that the formation of OCS from *cis*-HOCS becomes endothermic on a surface because of the large adsorption energy of the HOCS intermediate.

Both *cis*- and *trans*-HOCS can also react with a hydrogen atom. Again, there is a chance of approximately 50% of H_2 + OCS formation, depending on the angle of approach of the hydrogen atom. When the hydrogen atom approaches from the wrong angle, H_2O and CS are formed instead. Reactions of HOCS + H are barrierless; thus again, the outcome of the reaction depends strongly on the collision geometry.

Previous work investigated the effect of coronene on CO_2 formation via pathways similar to those described here which lead to the formation of OCS.[38] OCS and CO_2 are isovalent, and therefore, comparison of the reactions can tell us about the difference in reactivity between oxygen and sulfur. The OH + CO reaction, which in the gas phase has a negative activation barrier of −0.7 kJ mol^{-1} to *trans*-HOCO formation, has an even more negative activation barrier of −1.9 kJ mol^{-1} on coronene. In comparison, the HS + CO barrier is reduced from +6.7 kJ mol^{-1} in the gas phase to +3.3 kJ mol^{-1} on coronene, and the CS + OH reaction has no barrier in either the gas phase or on coronene. A possible explanation for the stronger catalytic behavior of the coronene surface for OCS formation than for CO_2 formation may be that the interaction of the more polarizable sulfur atom with the surface is stronger than that of oxygen, which leads to an increased stabilization of the OCS transition state by the coronene model surface.

4. Summary and Conclusions

This study of the formation of OCS via four different reaction pathways in the gas phase and on a coronene model surface has shown that coronene has a catalytic influence on OCS formation reactions. Activation barriers are reduced from 18.7 kJ mol^{-1} in the gas phase to 7.1 kJ mol^{-1} (ER mechanism) for the CO + ^{3}S $\rightarrow$^{3}OCS reaction, from 15.4 kJ mol^{-1} in the gas phase to 9.3 kJ mol^{-1} (HA mechanism) for the reaction of CO + HS, or disappear entirely (CS + ^{3}O $\rightarrow$^{3}OCS, CS + OH). This has the potential to speed up these reactions considerably in the ISM. For two reaction pathways, CO + ^{3}S and CO + HS, the most important role of the surface is the reduction in activation energy, without which the barriers are too high and the reactions will not contribute significantly to OCS formation in the ISM. All species are physisorbed, which not only reduces the activation barrier but also allows reactants and products to diffuse on a surface and eventually to desorb back into the gas phase. Excited oxygen and sulfur (^{1}O and ^{1}S) will be too strongly bound for further reactions to occur, because they are chemisorbed on coronene. However, they can yield OCS via direct reaction with CS or CO, respectively, if they do not thermally equilibrate with the surface (the HA mechanism).

The ^{3}S + CO reaction 1 is the most strongly catalyzed reaction, with the activation barrier reduced from 18.7 kJ mol^{-1} in the gas phase to 7.1 kJ mol^{-1} with the reaction becoming exothermic on coronene, thus potentially contributing to OCS formation in the ISM. Coronene catalyzes the formation of both *cis*- and *trans*-HSCO, reaction 2. The *trans*-form is strongly favored, and by assuming that the pre-exponential factors do not differ too much, no *cis*-HSCO will be formed. Once *trans*-HSCO is formed and stabilized on the dust grain surface, it can react with another species, probably a hydrogen atom, forming H_2 and OCS or H_2S and CO, depending on how the hydrogen atom approaches the HSCO radical.

The CS + O reaction 3 is also catalyzed, and the negative activation barrier in the gas phase could not be located for the surface reaction. As with reaction 4, OH + CS, the main catalytic effect of the surface is to absorb the excess formation energy before the reaction continues to yield CO and S or CO and HS.

In dark clouds between stars, exactly which OCS formation routes are viable depends on both the rate of the reaction at interstellar temperatures and the local concentration of reactants. The most favorable reaction in the ISM is therefore not exclusively dependent on activation barriers but also on the availability of the specific reactants required.

In previous research on CO_2-formation,[38] it was shown that the ER mechanism is usually favored over the LH mechanism, for two reasons. First, the gas-phase activation barriers are more catalyzed in the ER case than they are in the LH case. Second, when no activation barrier is present, the diffusion barrier effectively plays this role in the LH case, where still no barrier is present in the ER case. However, because dust grains can physisorb the reactants and because the relative abundances of sulfur-bearing species are much smaller than the abundance of O, OH, and water (the reactants in CO_2 formation), the LH or HA reactions are dominant over the ER mechanism for OCS formation. Because, in addition, species can and will reside on dust grains for very long time scales, the HA mechanism is less likely than the LH mechanism. We conclude therefore that the LH mechanism is the most probable in the ISM, because the activation barriers are clearly strongly catalyzed and low enough to be overcome in dark, molecular clouds.

Acknowledgment. The EPSRC is acknowledged for funding for D.A.A., for a postdoctoral fellowship for T.P.M.G. (EP/D500524), and for computer resources on HPCx used through the Materials Chemistry Consortium (EP/D504872) and the U.K. Car−Parrinello consortium. We also thank the National Service for Computational Chemistry Software for use of their computer resources. Serena Viti is acknowledged for many interesting discussions and suggestions concerning OCS formation. This work forms part of the research currently being undertaken in the UCL Centre for Cosmic Chemistry and Physics.

References and Notes

(1) Williams, D. A. *Faraday Discuss.* **1998**, *109*, 1.
(2) Williams, D. A.; Taylor, S. D. Q. J. *Roy. Astron. Soc.* **1996**, *37*, 565.
(3) Greenberg, J. M. *Surf. Sci.* **2002**, *500*, 793.
(4) Hu, A. M.; Duley, W. W. *Astrophys. J.* **2007**, *660*, L137.
(5) Williams, D. A. *Surf. Sci.* **2002**, *500*, 823.
(6) Williams, D. A.; Brown, W. A.; Price, S. D.; Rawlings, J. M. C.; Viti, S. *Astron. Geophys.* **2007**, *48*, 25.
(7) Pirronello, V.; Liu, C.; Shen, L. Y.; Vidali, G. *Astrophys. J.* **1997**, *475*, L69.
(8) Garrod, R.; Park, I. H.; Caselli, P.; Herbst, E. *Faraday Discuss.* **2006**, *133*, 51.
(9) Vidali, G.; Roser, J. E.; Manico, G. et al. Experimental study of the formation of molecular hydrogen and carbon dioxide on dust grain analogues. *Space Life Sciences: Steps toward Origins of Life*; 2004; Vol. 33; p 6.
(10) Vidali, G.; Roser, J. E.; Ling, L.; et al. *Faraday Discuss.* **2006**, *133*, 125.
(11) Fraser, H. J.; Bisschop, S. E.; Pontoppidan, K. M.; Tielens, A.; G, G. M.; van Dishoeck, E. F. *Mon. Not. R. Astron. Soc.* **2005**, *356*, 125.
(12) Watanabe, N.; Nagaoka, A.; Shiraki, T.; Kouchi, A. *Astrophys. J.* **2004**, *616*, 638.
(13) Galano, A. *J. Phys. Chem. A* **2007**, *111*, 1677.
(14) Bonfanti, M.; Martinazzo, R.; Tantardini, G. F.; et al. *J. Phys. Chem. C* **2007**, *111*, 5825.
(15) Xu, S.; Irle, S.; Musaev, A. G.; Lin, M. C. *J. Phys. Chem. A* **2005**, *109*, 9563.
(16) Mendoza, C.; Ruette, F.; Martorell, G.; Rodriguez, L. S. *Astrophys. J.* **2004**, *601*, L59.
(17) Morisset, S.; Aguillon, F.; Sizun, M.; Sidis, V. *Phys. Chem. Chem. Phys.* **2003**, *5*, 506.
(18) Forte, G.; Grassi, A.; Lombardo, G. M.; La Magna, A.; Angilell, G. G. N.; Pucci, R.; Vilardi, R. *Phys. Lett. A* **2008**, *372*, 6168.
(19) Codella, C.; Viti, S.; Williams, D. A.; Bachiller, R. *Astrophys. J.* **2006**, *644*, L41.
(20) Greenwood, E. *Chemistry of the Elements*; Butterworth Heinemann, 2001.
(21) Gibb, E. L.; Whittet, D. C. B.; Schutte, W. A.; Boogeert, A. C. A.; Chiar, J. E.; Ehrenfreund, P.; Gerakines, P. A.; Keane, J. V.; Tielens, A. G. G. M.; van Dishoeck, E. F.; Kerkhof, O. *Astrophys. J.* **2000**, *536*, 347.
(22) Boogert, A. C. A.; Tielens, A. G. G. M.; Ceccarelli, C.; Boonman, A. M. S.; van Dishoeck, E. F.; Keane, J. V.; Whittet, D. C. B.; de Graauw, T. *Astron. Astrophys.* **2000**, *360*, 683.
(23) Palumbo, M. E.; Geballe, T. R.; Tielens, A. G. G. M. *Astrophys. J.* **1997**, *479*, 839.
(24) Codella, C.; Bachiller, R.; Benedettini, M.; Caselli, P.; Viti, S.; Wakelam, V. *Mon. Not. R. Astron. Soc.* **2005**, *361*, 244.
(25) Hijazo, J.; Gonzales, M.; Sayós, R.; Novoa, J. J. *Chem. Phys. Lett.* **1994**, *222*, 15.
(26) Rice, B. M.; Cartland, H. E.; Chabalowski, C. F. *Chem. Phys. Lett.* **1993**, *211*, 283.
(27) Rice, B. M.; Chabalowski, C. F. *J. Phys. Chem.* **1994**, *98*, 9488.
(28) Rice, B. M.; Pai, S. V.; Chabalowski, C. F. *J. Phys. Chem. A* **1998**, *102*, 6950.
(29) Sayós, R.; Gonzalez, M.; Aguilar, A. *Chem. Phys.* **1990**, *141*, 401.
(30) Gonzales, M.; Hijazo, J.; Novoa, J. J.; Sayós, R. *J. Chem. Phys.* **1996**, *105*, 10999.
(31) Häusler, D.; Rice, J.; Wittig, C. *J. Phys. Chem.* **1987**, *91*, 5413.
(32) Ferrante, R. F.; Moore, M. H.; Spiliotis, M. M.; Hudson, R. L. *Astrophys. J.* **2008**, *684*, 1210.
(33) Lo, W. *J. Chem. Phys.* **2004**, *120*, 5717.
(34) UMIST database for astrochemistry, www.udfa.net.
(35) Frisch, M. J.; Trucks, G. W.; Schlegel, H. B. et al. Gaussian, Inc.: Wallingford CT, 2004.
(36) Werner, H. J. et al. 2008, MOLPRO version 2008.1, a package of ab initio programs.

(37) Zhao, Y.; Truhlar, D. G. *J. Phys. Chem. A* **2004**, *108*, 6908.

(38) Goumans, T. P. M.; Uppal, M. A.; Brown, W. A. *Mon. Not. R. Astron. Soc.* **2008**, *384*, 1158.

(39) Zhongxiang, Z. *J. Phys. Org. Chem.* **1995**, *8*, 103.

(40) Cioslowski, J.; O'Connor, P. B.; Fleischmann, E. D. *J. Am. Chem. Soc.* **1991**, *113*, 1086.

(41) Latimer, E. R.; Islam, F.; Price, S. D. *Chem. Phys. Lett.* **2008**, *455*, 174.

(42) Lilenfeld, H. V.; Richardson, R. J. *J. Chem. Phys.* **1977**, *67*, 3991.

(43) Gurvich, L. V.; Veyts, I. V.; Alcock, C. B. Hemisphere Pub. Co.: New York, 1989.

(44) Cox, J. D.; Wagman, D. D.; Medvedev, V. A. Hemisphere; New York, 1989.

(45) Eland, J. H. D.; Berkowitz, J. *J. Chem. Phys.* **1979**, *70*, 5151.

(46) Herzberg, G. *Electronic spectra and electronic structure of polyatomic molecules*; Van Nostrand: New York, 1966.

(47) Shapiro, M.; Halavee, U. *Chem. Phys. Lett.* **1976**, *40*, 387.

(48) Oldershaw, G. A.; Porter, D. A. J. *Chem. Soc. Faraday Trans.* **1972**, *68*, 709.

(49) Tsunashima, S.; Yokota, T.; Safarik, I.; Gunning, H. E.; Strausz, O. P. *J. Phys. Chem.* **1975**, *79*, 775.

(50) Piper, J.; Morrison, J. A.; Peters, C. *Mol. Phys.* **1984**, *53*, 1463.

(51) Burke, D. J.; Brown, W. A. *Phys. Chem. Chem. Phys.* submitted.

(52) Karimi, M.; Vidali, G. *Surf. Sci.* **1989**, *208*, L73.

(53) Mattera, L.; Rosatelli, F.; Salvo, C.; Tommasini, F.; Valbusa, U.; Vidali, G. *Surf. Sci.* **1980**, *93*, 515.

(54) Goumans, T. P. M.; Wander, A.; Catlow, C. R. A.; Brown, W. A. *Mon. Not. R. Astron. Soc.* **2007**, *382*, 1829.

(55) Goumans, T. P. M.; Catlow, C. R. A.; Brown, W. A. *J. Phys. Chem. C* **2008**, *112*, 15419.

(56) Gail, H. P.; Sedlmayr, E. *Astron. Astrophys.* **1975**, *41*, 359.

(57) Greenwald, E. E.; North, S. W.; Georgievskii, Y.; Klippenstein, S. J. *J. Phys. Chem. A* **2005**, *109*, 6031.

(58) Sabbah, H.; Biennier, L.; Sims, I. R.; Georgievskii, Y.; Klippenstein, S. J.; Smith, I. W. M. *Science* **2007**, *317*, 102.

(59) Smith, I. V. M. *Angew. Chem.* **2006**, *45*, 2842.

(60) Sabbah, H.; Binnier, L.; Sims, I. R.; Georgievskii, Y.; Klippenstein, S. J.; Smith, I. V. M. *Science* **2007**, *317*, 102.

(61) Georgievskii, Y.; Klippenstein, S. J. *J. Phys. Chem. A* **2007**, *111*, 3802.

JP9083212